UC Santa Cruz
UC Santa Cruz Previously Published Works

Title

Migratory earthquake precursors are dominant on an ice stream fault.

Permalink

https://escholarship.org/uc/item/32x6h4z0

Journal

Science Advances, 7(6)

Authors

Barcheck, G

Brodsky, Emily

Fulton, P

et al.

Publication Date

2021-02-01

DOI

10.1126/sciadv.abd0105

Peer reviewed

GEOLOGY

Migratory earthquake precursors are dominant on an ice stream fault

G. Barcheck[1]*, E. E. Brodsky[2], P. M. Fulton[1], M. A. King[3], M. R. Siegfried[4], S. Tulaczyk[2]

Simple fault models predict earthquake nucleation near the eventual hypocenter (self-nucleation). However, some earthquakes have migratory foreshocks and possibly slow slip that travel large distances toward the eventual mainshock hypocenter (migratory nucleation). Scarce observations of migratory nucleation may result from real differences between faults or merely observational limitations. We use Global Positioning System and passive seismic records of the easily observed daily ice stream earthquake cycle of the Whillans Ice Plain, West Antarctica, to quantify the prevalence of migratory versus self-nucleation in a large-scale, natural stick-slip system. We find abundant and predominantly migratory precursory slip, whereas self-nucleation is nearly absent. This demonstration that migratory nucleation exists on a natural fault implies that more-observable migratory precursors may also occur before some earthquakes.

INTRODUCTION

Seismology has reached a crossroads in the conceptual understanding of how earthquakes start. Early work on simple homogeneous faults modeled precursory processes as self-nucleation or small regions of precursory slip in the same place as the ultimate earthquake hypocenter (1, 2). Such small nucleation zones would cause limited precursory deformation and be challenging to use for earthquake prediction (2). However, recent observations suggest that in natural faults, some earthquakes may begin as migrating slow slip that traverses a large area before reaching the eventual earthquake hypocenter (3–6). Migrating foreshocks and precursory slow slip before the 2011 M9.1 Tohoku and 2014 M8.1 Iquique earthquakes suggest that this alternative, potentially more observable migratory nucleation style may occur in some cases (5, 6). Such migratory precursory sequences are rarely recorded, but it is unknown whether the observational paucity results from real physical differences between faults or merely instrumental limitations. Identifying whether earthquakes tend to start with migratory versus self-nucleation remains an outstanding problem with implications for understanding the abundance and potential resolvability of earthquake precursors.

We address this uncertainty in how earthquakes nucleate by examining the precursory slip behavior of multiple large-scale ice stream earthquakes beneath the Whillans Ice Plain, West Antarctica. Our new approach to understanding earthquake initiation uses a large, stick-slipping ice stream as a fault-scale analog to slip on tectonic faults, complementing laboratory-scale studies that can approximate fault stresses but not scale. The Whillans Ice Plain, at the downstream confluence of two major ice streams draining the West Antarctic Ice Sheet (Fig. 1), exhibits a stick-slip cycle with moment magnitude (M_w) ~ 7 ice stream earthquakes once or twice every day (7). These earthquakes radiate long-period (30 to 180 s) seismic waves (8–10) and involve up to ~0.75 m of slip along the ice stream basal fault over ~30 min and across an area ~100 × 150 km (11).

Together with the shallow slip surface (<1 km) and low rupture speeds (0.1 to 1.5 km/s) (9, 12), the characteristics of these ice stream earthquakes make them much easier to observe than typical tectonic earthquakes. Here, we present on-ice geodetic and seismic observations that reveal migratory nucleation as the dominant nucleation process of ice stream earthquakes, and we discuss the implications for understanding earthquake precursors in other settings.

The Whillans stick-slip cycle is driven by elastic strain accumulation from continuous upstream ice motion on a large locked central asperity (high geodetic coupling region; Fig. 1) that is surrounded by slowly sliding ice (Fig. 1) (13, 14). This "central asperity" corresponds to a shallow (~100 m) basal topographic high that may route subglacial water away and result in locally higher normal stress (15). Ice stream earthquakes occur when sudden failure at the ice base rapidly ruptures this central asperity, causing the ice to begin sliding faster, and rupture propagates across the entire fault over ~10 min (11). The ice stream earthquakes are generally slip predictable and systematic, with both displacement and peak slip velocity scaling with recurrence time (Fig. 2) (13, 16). However, tidal cycles beneath the nearby floating Ross Ice Shelf modulate longitudinal stresses and event timing (7, 11). The epicenters of these large-scale M_w ~ 7 ice stream earthquakes have previously been found to correspond to one of two different common locations (9): High-speed slip tends to start at a Central epicenter (purple star, Fig. 1) at the upstream end of the high geodetic coupling patch or a Grounding Zone epicenter (yellow star, Fig. 1) where stress concentrations from tidal flexure and strain gradients between grounded and floating ice may help promote rapid rupture. Failure at the Grounding Zone epicenter can reach dynamic speeds that radiate seismic energy (9, 12).

In this work, we focus on how these ice stream earthquakes begin. A several-minutes-long period of slow precursory slip was previously noted near the Central epicenter before some ice stream earthquakes (17) and was thought to occur in about the same region that high-speed slip begins, which would be a record of self-nucleation. Here, we use on-ice Global Positioning System (GPS) instruments to resolve where this precursory slow slip phase occurs relative to where the high-speed slip begins for 75 ice stream earthquakes. We show that slow precursory slip is common before ice stream earthquakes, and, in contrast to the previous interpretation, we demonstrate that precursory slip is predominantly migratory, and self-nucleation is rare

[1]Department of Earth and Atmospheric Sciences, Cornell University, 112 Hollister Drive, Ithaca, NY 14853-1504, USA. [2]Department of Earth and Planetary Sciences, University of California, Santa Cruz, 1156 High Street, Santa Cruz, CA 95064, USA. [3]Geography and Spatial Sciences, University of Tasmania, Hobart, Tasmania 7001, Australia. [4]Department of Geophysics, Colorado School of Mines, Golden, CO 80401, USA.
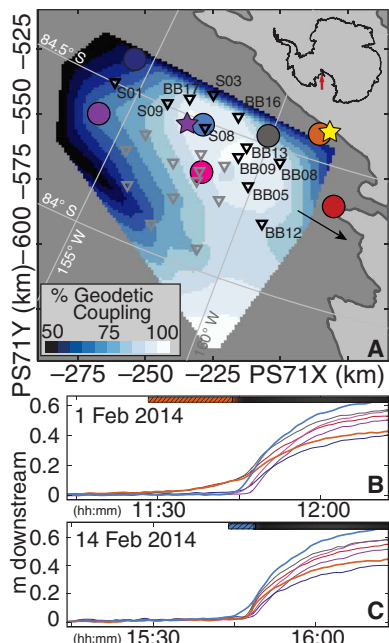*Corresponding author. Email: grace.barcheck@cornell.edu

Fig. 1. Map of Whillans Ice Plain and example ice stream earthquakes showing slow precursory slip. (**A**) Map of Whillans Ice Plain. Dark gray in background indicates grounded ice and light gray is floating ice. Darker gray line is the grounding line (*22*). The geodetic coupling overlay reflects the percent of total ice surface motion accommodated during ice stream earthquakes (*14*). Circles indicate GPS sites used. Important GPS proximal to the Central and Grounding Zone epicenters are light blue and orange, respectively. Stars are locations of the Central (purple) and Grounding Zone (yellow) epicenters (*9*). Triangles show broadband seismometer locations, with black triangles and labels indicating sites with data shown in Fig. 4. Black arrow shows ice flow direction at Central (blue) GPS. Map coordinates are in Antarctic Polar Stereographic (PS71). (**B**) Downstream displacement at all GPS during a type I event. Slow precursory slip occurs in a grounding zone proximal region [orange, red, and gray circles in (A) and same-colored lines in (B)], and high-speed slip is seen first at the Central GPS (light blue), indicating that high-speed slip began at the Central epicenter (purple star, A). (**C**) Downstream displacement at all GPS during a type II event. Slow precursory slip occurs near the Central GPS (light blue), and high-speed slip is seen first at the Grounding Zone GPS (orange), indicating that high-speed slip began at the Grounding Zone epicenter (yellow star, A). Hatched, colored bars in (B) and (C) show approximate duration of precursory motion at the correspondingly colored GPS, and the black bar shows approximate duration of ice stream earthquake, with onset of high-speed slip at the start.

for ice stream earthquakes. The data imply that at least some natural systems are capable of a more observable migratory style of earthquake initiation.

RESULTS

At seven on-ice continuous GPS stations, we recorded ice motion for 2 months in early 2014, capturing 75 ice stream earthquakes (Fig. 1). We positioned a station near each of the two epicenters (light blue and orange circles, Fig. 1), which allows us to determine which epicenter high-speed slip begins at. Nearly all ice stream earthquakes in the dataset (73 of 75, 97%; table S1) exhibit a period of slow precursory motion lasting minutes to hours in one of two regions: sometimes near the Central epicenter GPS (10 events, 13%; light blue GPS, Fig. 1; occasionally purple, pink, and dark blue GPS) or, more often, in a tens of kilometers wide region downstream of the
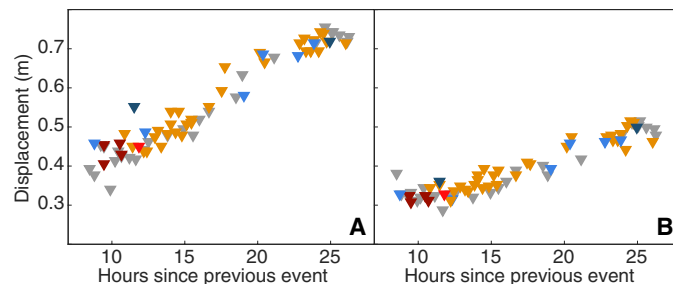

Fig. 2. Slip predictability of ice stream earthquakes. Total displacement during each ice stream earthquake in the dataset as a function of recurrence time. (**A**) Displacement at the Central GPS (light blue circle, Fig. 1). (**B**) Displacement at the Grounding Zone GPS (orange circle, Fig. 1). (A and B): Colors correspond to event types described in Table 1.

central asperity that includes the Grounding Zone epicenter (46 events, 61%; orange, red, and gray GPS, Fig. 1). Occasionally, slow precursory slip is observed in both regions (17 events, 22%), although the precursors occur in a particular sequence, with the Grounding Zone region always starting to move first. Three GPS stations in the Grounding Zone region (orange, red, and gray, Fig. 1) show that precursory slip in that region occurs nearly synchronously over tens of kilometers, and there is no evidence of residually coupled patches within this slipping region.

Using data from these seven GPS, we categorize events into six dominant types (Table 1) based on which of the two regions exhibits slow quasi-static slip and which of the two epicentral GPS enters the high-speed unstable slip phase first. Most ice stream earthquakes (42 events, 56%; types I and II defined in Table 1) have precursory quasi-static slip in either the Central or Grounding Zone precursory region and high-speed unstable slip that first occurs at the opposite epicenter GPS (Fig. 3, A to H). This pattern suggests that the precursory slip begins in one region and migrates across the ice plain, loading and triggering high-speed slip at the opposite epicenter. An additional 5% of events (four events; type IIIa) are "super-migratory," showing slow precursory slip first over several hours in the Grounding Zone region, then at the Central GPS, and lastly showing high-speed unstable slip first at the Grounding Zone epicenter GPS (Fig. 3, I to M). Super-migratory precursory sequences appear to migrate across the ice plain twice before triggering high-speed slip. In total, 61% of the dataset (46 events; types I, II, and IIIa) has evidence for a migratory precursory process. In contrast, only 3% of the dataset (two events; types IIIb, IV, and V) shows evidence for nonmigratory nucleation. The remaining 36% of ice stream earthquakes (27 events) has a nondeterminable precursory sequence, primarily at shorter interevent times when peak slip velocity is lower and the onset of high-speed slip is therefore more difficult to identify in the noisy velocity records. This dominant pattern of precursory motion occurring in a region separated from the onset of high-speed unstable slip implies that migratory precursory processes are characteristic of Whillans ice stream earthquakes, apparently regardless of where the precursory slip occurs or which epicenter eventually fails during high-speed slip onset.

Complementary data from a larger network of broadband seismometers operated on the Whillans Ice Plain for 17 days in December 2010 (triangles, Fig. 1) (*9*, *12*, *13*) confirm the migratory nature of precursory slip before five earlier ice stream earthquakes (Fig. 4). Minimally processed broadband seismic velocity records

Table 1. Definitions of ice stream earthquake types and counts of events per category. Colors in left-hand column correspond to symbol colors in Fig. 2.

Color Fig. 2	Event type	Region with precursory slip	GPS location with fast slip first	Number in dataset [%]	
	I	Grounding Zone	Central	35 [47%]	Evidence of migratory nucleation n = 46 (61%)
	I	Grounding Zone, >~45 min	Central	1 [1%]	
	II	Central	Grounding Zone	6 [8%]	
	IIIa	Grounding Zone, >~45 min, and then Center also	Grounding Zone	4 [5%]	
	IIIb	Grounding Zone	Grounding Zone	0 [0%]	Evidence of nonmigratory nucleation n = 2 (3%)
	IV	Central	Central	0 [0%]	
	V	None	Same time	2 [3%]	
	Cannot determine	Grounding Zone or Central	Cannot tell	27 [36%]	Ambiguous n = 27 (36%)

show a distinct long-period negative excursion on the East component (approximately the ice flow direction) lasting minutes to tens of minutes immediately before each ice stream earthquake begins (Fig. 4, A and B). We interpret this seismic precursor as resulting from slow basal slip and suggest that it represents the same precursory sliding we observe with GPS. This interpretation is supported by occasional observation of coincident slow precursory motion observable a few minutes later on collocated GPS (Fig. 4, A and B), as well as coincident basal icequakes beneath seismic site S08 during two of the five precursors (Fig. 4, C and D, and fig. S7). Basal icequakes are a strong indicator of slip on the basal fault and are comparable to foreshock sequences indicating slow slip before some tectonic earthquakes (5, 6).

Five events from this 2010 seismic dataset show clear migration of the broadband seismic precursor (tan areas, Fig. 4, E and F, and fig. S7), generally appearing first at site S08 for ~5 to 15 min, before migrating to sites primarily downstream at an expansion rate of ~75 to 125 m/s. For all five events, eventual high-speed unstable slip was previously shown to begin at the Grounding Zone epicenter at a time later than the seismic precursor (gray dashed lines, Fig. 4) (9) and after the precursor has migrated toward that region. We interpret this systematic precursory sequence as a slowly migrating region of basal fault slip that begins near site S08 at the upstream end of the central asperity and expands approximately downstream, eventually reaching and triggering dynamic unstable slip at the Grounding Zone epicenter. This sequence is compatible with either type II or IIIa events, in which precursory slip near the Central GPS triggers high-speed slip at the Grounding Zone GPS.

The GPS observations reveal that precursory slip is a dominant feature of the ice stream earthquake cycle, and seismic data confirm that it is migratory. We find that migratory nucleation is typical, and self-nucleation is rare for these ice stream earthquakes, which has valuable implications for understanding tectonic earthquake initiation on heterogeneous faults.

DISCUSSION
The Whillans Ice Plain is a valuable natural laboratory for studying earthquake nucleation because, in addition to having a short recur-

rence time and easily observed rupture propagation, its stick-slip cycle is controlled by the same physical processes as tectonic earthquakes: elasticity and friction. Despite ice viscoelasticity (13, 18), continued elastic stress accumulation on the central asperity over periods up to at least ~26 hours is demonstrated by the slip predictability of ice stream earthquakes, in which longer interevent times and greater stress accumulation result in proportionally larger slip (Fig. 2). The ice stream fault is also well described as a frictional interface, with debris-rich basal ice (19, 20) sliding across a meters-thick layer of deformable till (15), the glacial equivalent of fault gouge. Sliding of debris-laden ice is shown to be rate weakening (21, 22), which is necessary for stick-slip, and widespread basal icequakes and tremor on the highly coupled central asperity support inferences of debris-rich basal ice and rate-weakening friction in that region (14).

There are also important differences between the ice stream and tectonic faults. The elastic modulus of ice is lower than rock, which means ice strains are larger than in rock for an equivalent stress. Ice stream fault overburden is also lower than in tectonic earthquake initiation zones, because ice has a lower bulk density than rock and the slip surface is <1 km deep. High basal pore pressures further lower effective normal stress on the ice stream fault surface, possibly to values as low as tens of kilopascals (23). Such low effective normal stress allows fast ice stream slip in ice sheets generally, and the Whillans basal fault is no exception. Whether comparable conditions exist on tectonic faults is uncertain, because the absolute level of stress on tectonic faults in the presence of pore pressure is the subject of an ongoing debate (24–26). These differences are evidently not fundamental, as both the ice stream and tectonic systems can evolve to a stick-slip configuration, only with different levels of slip and stress. A more substantial difference is the thin sheet geometry of the Whillans fault, with ice <1 km thick over a ~100-km-wide fault, which limits the transmission of stress over large distances and therefore the elastic energy release rate during fault rupture (12). For small to moderate earthquakes, faults can draw elastic energy from a volume around the fault that is substantially larger than the rupture dimension, which is different from the ice stream fault. The largest earthquakes, however, also have geometrically limited volumes from which to draw energy, especially in the case of shallow portions of subducting slabs.
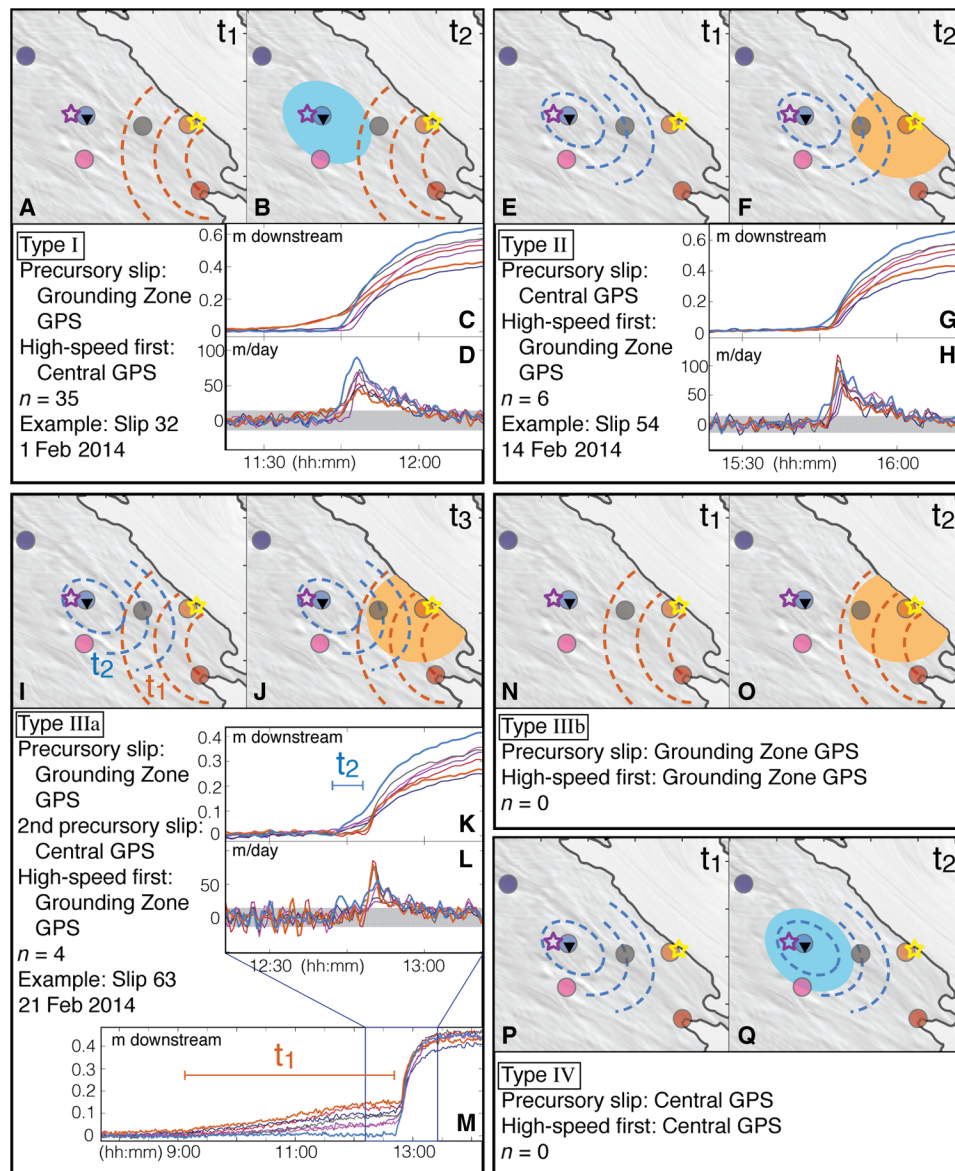
Fig. 3. Cartoon illustrations, example GPS data, and counts of dominant ice stream earthquake rupture types from Table 1. (**A**, **B**, **E**, **F**, **I**, **J**, **N**, **O**, **P**, and **Q**) In cartoons, stars and circles correspond to epicenters and GPS locations from Fig. 1, and the dark gray line is the grounding line (*22*). Black triangle indicates seismic site S08. Dashed lines indicate precursory slip starting near the same-colored GPS. Solid colors indicate the main phase of high-speed unstable slip starting at same-colored GPS. The top panel of the GPS data (**C**, **G**, and **K**) is displacement in the downstream direction, and the bottom panel (**D**, **H**, and **L**) is the same data differentiated to velocity. (**M**) The same data as (K) over a longer time span. Downstream displacement in (K) has been normalized to zero at 45 min before the ice stream earthquake. GPS data color corresponds to site colors in Fig. 1. Gray bars indicate the velocity range spanning the middle 90% of velocity values.

An important major similarity between the ice stream and tectonic faults is spatial heterogeneity, which is critical to understanding why and where migratory nucleation might occur instead of self-nucleation. Ice stream frictional heterogeneity is revealed by patterns in basal icequake occurrence at scales of both tens of kilometers (*14*) and sub-kilometer (*27*), and heterogeneity in elastic strain accumulation between events is shown by the geodetic coupling field (Fig. 1) (*13*, *14*)). On such a heterogeneous fault surface, the condition to initiate accelerated slow slip is not necessarily the same as the condition to initiate rapid, dynamic slip. Slip accelerated above the background rate initiates when the imposed shear stress exceeds the

local frictional failure criterion, a condition that will be reached in some region(s) of a heterogeneous fault first, and not others. Such a slipping region can expand but will do so only slowly as long as the elastic energy release rate G of the expanding rupture front is only marginally higher than the dissipative processes (*28*). This is likely the case for slow expanding precursory slip before ice stream earthquakes (for example, Fig. 4). For a slowly expanding rupture to then accelerate to dynamic speeds requires an increase in elastic energy release rate relative to dissipative processes. Evidently, both epicentral regions of the Whillans fault have adequate prestress to cause slow rupture front expansion and precursory slow slip, but neither
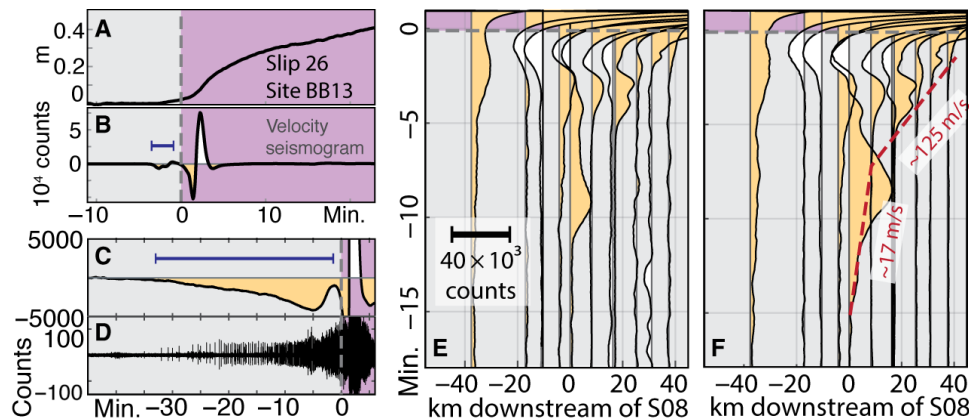
Fig. 4. Broadband seismic evidence of a migrating long-period precursor showing migrating basal slip. (**A**) GPS downstream displacement and (**B**) corresponding broadband seismic data at site BB13 for event no. 26, starting 20:36, 30 December 2010 (*9*). Note the small precursory negative seismic excursion (blue bar). (**C**) Minimally processed seismic data from site S08, event no. 1 [starting 12:50, 14 December 2010 (*9*)], with a ~30-min-long negative long-period precursor (blue bar). (**D**) Same data with a 10- to 50-Hz bandpass filter applied, showing abundant basal icequakes, indicating that basal slip is occurring. (**E** and **F**) Two examples of spatial migration of the long-period seismic precursor, event no. 14, starting 01:01, 23 December 2010 (E), and event no. 7, starting 22:45, 18 December 2020 (F) (*9*). Black lines are minimally processed East component seismic data, rotated vertically and offset along the *x* axis by distance downstream of site S08. Tan fill indicates negative data, emphasizing the broadband seismic precursor. As plotted, seismic data go off-scale following onset of high-speed slip. Red dashed lines and values in (F) indicate approximate onset of long-period negative seismic precursor and approximate migration rates along flow. (All) Gray dashed line is the high-speed slip origin time (*9*). Duration of main ice stream earthquake is purple, with other data overlaid.

by itself can generate a high-enough energy release rate to accelerate the rupture to high speeds unless a migratory slip event loads it further.

Our finding that both epicentral regions can exhibit both slow precursory slip and high-speed dynamic slip implies that variable loading conditions and corresponding spatially variable elastic strain accumulation between consecutive events control where slow and fast slip initiate for ice stream earthquakes rather than fault frictional properties. Although it is possible that the epicenters are defined by frictional differences from the rest of the fault, the observation that the location of high-speed slip onset can switch rapidly between consecutive events further implicates tidally varying loading rather than frictional variability.

For the Whillans observations, we suggest that when the precursory slip propagates from one epicentral region to the other, the delivery of additional strain energy by the migrating precursory slip to the opposite, still-stressed region causes the energy release rate to increase past some critical threshold. The rupture can then expand unstably, in some cases becoming fully dynamic and radiating seismic energy (*8*–*10*), and tap large-scale stresses on the central asperity. This results in rupture propagation across the entire Whillans Ice Plain fault, including rerupture and continued slip of regions of previous precursory motion. This observation from a large-scale natural stick-slip system is consistent with the ignition-limited earthquake initiation model suggested in (*4*) on the basis of laboratory experiments, in which a "kick" from surrounding slow slip can cause dynamic failure of an isolated asperity that otherwise cannot nucleate dynamic rupture at the current conditions.

Extrapolating this model to heterogeneous tectonic faults, migratory nucleation may be possible where elastic energy release rate *G* of an accelerated slipping region remains low despite rupture of a large fault area. Dynamic rupture can then initiate if rupture propagates into a region capable of larger stress release, which drives the energy release rate beyond the limiting threshold. Heterogeneity may also be a mechanism to limit *G*, by creating energy sinks and

barriers to fast rupture expansion (*3*). As nearly all tectonic faults have variable lithology, pore pressure, and frictional conditions, tectonic faults are likely at least as heterogeneous as the Whillans fault and, therefore, potentially as prone to migratory nucleation caused by limited elastic energy release rate *G*. How migratory nucleation scales from the ice stream to tectonic faults is an outstanding question and depends on poorly constrained fault zone conditions. An important caveat to generalization comes from the likely difference in absolute stress between Whillans and tectonic faults. The low normal stress of the Whillans Ice Plain might reinforce the tendency of a heterogeneous system to exhibit migratory nucleation. If stress drops are complete, as suggested by the slip predictability of ice stream earthquakes, then low ice stream normal stress limits the stress drops and thus elastic energy release rate *G*. By comparison, tectonic faults that also operate at low normal stress could also be likely to exhibit migratory nucleation.

These observations of repeated precursory signals before ice stream earthquakes reveal that migratory earthquake nucleation is dominant compared to self-nucleation on this large-scale, natural ice stream fault. The predominance of this behavior challenges simple earthquake self-nucleation models developed for homogeneous faults (*1*, *2*) and implies that large-scale migratory precursors may be expected on some natural faults. The expectation of migratory nucleation before earthquakes can fundamentally affect strategies for searching for earthquake precursors: Earthquake prediction efforts focused on observing local, small-scale creep (*2*) should be supplemented with strategies to understand and observe large slip regions far from the eventual hypocenter, especially in regions inferred to have low effective normal stress or high heterogeneity.

The apparent lack of self-nucleation in the large-scale Whillans ice stream earthquakes cycle may result from properties and conditions within this system that control the threshold in *G* necessary for dynamic slip to occur. These results therefore likely have particular relevance for understanding subduction zones where slow unstable slip events that do not develop into dynamic earthquakes are now

commonly observed across multiple scales (*29*, *30*). Our findings suggest that these slow slip events may be capable of becoming dynamic earthquakes if they propagate into asperities that release relatively large amounts of stress, even if those same asperities sometimes have slow slip. Although the possibility of slow slip events triggering large earthquakes has been a major motivation for their study (*31*), the observation of migratory nucleation as the typical behavior of a large-scale, natural system is new and particularly important in fault regions where migratory nucleation may control whether a single asperity slips rapidly or slowly.

Last, our observations may have important glaciological implications, particularly for understanding the role that strong asperities—which are called sticky spots in the glaciological literature—play in the Marine Ice Sheet Instability (MISI), in which grounding line retreat into increasingly deep oceanic basins results in rapid increase in ice flux into the ocean and rapid sea level rise (*32*). We note that most (63 of 75) of the ice stream earthquakes in this dataset begin with a period of slow precursory slip near the Grounding Zone GPS, regardless of whether we can resolve where high-speed slip begins. The dominance of this process implies that grounding zone stress fluctuations can trigger pulses of increased ice slip rate and transmit stresses elastically many kilometers inland in a matter of minutes, causing fracture-like basal failure and sudden unstable slip of an otherwise notably strong asperity or sticky spot. This raises a concerning prospect, that migrating slip pulses generally can concentrate stress and cause elastic, fracture-like failure of upstream sticky spots that are thought to be otherwise critical for mitigating ice mass loss during the progression of the MISI in West Antarctica (*33*, *34*). Such fault-like behavior is currently not incorporated into glaciological models used to predict future marine-based ice mass balance. Further work is required to determine how widespread such accelerated migrating slip pulses may be.

MATERIALS AND METHODS

For our analysis, we first analyze data from seven on-ice continuous GPS stations that describe ice motion at 30-s sampling intervals for 2 months in early 2014. The time series captures 75 ice stream earthquakes, and data from GPS stations (light blue and orange circles, Fig. 1) near each epicenter (purple and yellow stars, Fig. 1) provide particularly useful constraints on where high-speed slip begins. The data are processed in kinematic mode using the *track* package (*35*), and we use a relatively high process noise [50 mm/$\sqrt{(\text{epoch})}$] to capture abrupt accelerations associated with unstable slip onset. The acausal smoothing feature is disabled during processing to avoid introducing artifacts that could be mistaken for ice stream earthquake precursory motion. Additional details of GPS processing are described in the Supplementary Materials.

Within the GPS data, nearly all the large ice stream earthquakes (73 of 75, 96%) exhibit a clearly resolvable period of slow precursory motion in one of two regions: sometimes near the Central epicenter GPS (light blue, Fig. 1) or, more often, in a grounding zone proximal region tens of kilometers wide downstream of the locked central asperity that includes the Grounding Zone epicenter (orange, red, and gray circles, Fig. 1).

Using ice surface velocity data from the seven GPS, we categorize events into six dominant types (Table 1) based on which of the two regions exhibits slow quasi-static slip and which of the two epicentral GPS enters the high-speed unstable slip phase first. An ice stream earthquake precursor is identified in GPS data as a relatively slow, low acceleration phase of GPS movement in the minutes to tens of minutes before an ice stream earthquake. Precursors are generally distinguished by lower slip velocity and acceleration than the primary, high-speed phase of the ice stream earthquake. The high-speed phase is, in turn, distinguished by a characteristic sudden and typically smooth, approximately linear increase in velocity that culminates in the peak velocity value. Any slip accelerated above the background rate before the onset of this sudden smooth velocity increase is judged to be a precursor.

Using a consistent set of criteria (described in the Supplementary Materials), we determine which of the two epicentral GPS (light blue or orange, Fig. 1) exhibits high-speed slip first as a proxy for the epicenter at which high-speed slip begins. Events are then categorized on the basis of where precursory and high-speed slip begin (Table 1). Events with precursory and high-speed slip beginning in different regions (types I, II, and IIIa) are evidence for migratory nucleation, while events with precursory and high-speed slip beginning in the same region are evidence of self-nucleation (types IIIb, IV, and V). Although the determination of precursory versus high-speed motion is somewhat subjective and this dataset contains nondeterminable examples, evaluating many repeats of ice stream earthquakes (75 events) circumvents much of this ambiguity.

SUPPLEMENTARY MATERIALS

REFERENCES AND NOTES

1. J. R. Rice, A. L. Ruina, Stability of steady frictional slipping. *J. Appl. Mech.* **50**, 343–349 (1983).
2. J. H. Dieterich, Earthquake nucleation on faults with rate- and state-dependent strength. *Tectonophysics* **211**, 115–134 (1992).
3. Y. Tal, B. H. Hager, J. P. Ampuero, The effects of fault roughness on the earthquake nucleation process. *J. Geophys. Res. Solid Earth* **123**, 437–456 (2018).
4. G. C. McLaskey, Earthquake initiation from laboratory observations and implications for foreshocks. *J. Geophys. Res. Solid Earth* **124**, 12882–12904 (2019).
5. S. Ruiz, M. Metois, A. Fuenzalida, J. Ruiz, F. Leyton, R. Grandin, C. Vigny, R. Madariaga, J. Campos, Intense foreshocks and a slow slip event preceded the 2014 Iquique M_w 8.1 earthquake. *Science* **345**, 1165–1169 (2014).
6. A. Kato, K. Obara, T. Igarashi, H. Tsuruoka, S. Nakagawa, N. Hirata, Propagation of Slow Slip Leading Up to the 2011 M_w 9.0 Tohoku-Oki Earthquake. *Science* **335**, 705–708 (2012).
7. R. Bindschadler, M. King, R. B. Alley, S. Anandakrishnan, L. Padman, Tidally controlled stick-slip discharge of a West Antarctic ice stream. *Science* **301**, 1087–1089 (2003).
8. D. A. Wiens, S. Anandakrishnan, J. P. Winberry, M. A. King, Simultaneous teleseismic and geodetic observations of the stick–slip motion of an Antarctic ice stream. *Nature* **453**, 770–774 (2008).
9. M. J. Pratt, J. P. Winberry, D. A. Wiens, S. Anandakrishnan, R. B. Alley, Seismic and geodetic evidence for grounding-line control of Whillans Ice Stream stick-slip events. *J. Geophys. Res. Earth Surf.* **119**, 333–348 (2014).
10. J. I. Walter, E. E. Brodsky, S. Tulaczyk, S. Y. Schwartz, R. Pettersson, Transient slip events from near-field seismic and geodetic data on a glacier fault, Whillans Ice Plain, West Antarctica. *J. Geophys. Res.* **116**, F01021 (2011).
11. J. P. Winberry, S. Anandakrishnan, R. B. Alley, R. A. Bindschadler, M. A. King, Basal mechanics of ice streams: Insights from the stick-slip motion of Whillans Ice Stream, West Antarctica. *J. Geophys. Res.* **114**, F01016 (2009).
12. J. I. Walter, I. Svetlizky, J. Fineberg, E. E. Brodsky, S. Tulaczyk, C. G. Barcheck, S. P. Carter, Rupture speed dependence on initial stress profiles: Insights from glacier and laboratory stick-slip. *Earth Planet. Sci. Lett.* **411**, 112–120 (2015).
13. J. P. Winberry, S. Anandakrishnan, R. B. Alley, D. A. Wiens, M. J. Pratt, Tidal pacing, skipped slips and the slowdown of Whillans Ice Stream, Antarctica. *J. Glaciol.* **60**, 795–807 (2014).
14. C. G. Barcheck, S. Tulaczyk, S. Y. Schwartz, J. I. Walter, J. P. Winberry, Implications of basal micro-earthquakes and tremor for ice stream mechanics: Stick-slip basal sliding and till erosion. *Earth Planet. Sci. Lett.* **486**, 54–60 (2018).
15. T. Luthra, S. Anandakrishnan, J. P. Winberry, R. B. Alley, N. Holschuh, Basal characteristics of the main sticky spot on the ice plain of Whillans Ice Stream, Antarctica. *Earth Planet. Sci. Lett.* **440**, 12–19 (2016).

16. M. R. Siegfried, H. A. Fricker, S. P. Carter, S. Tulaczyk, Episodic ice velocity fluctuations triggered by a subglacial flood in West Antarctica. *Geophys. Res. Lett.* **43**, 2640–2648 (2016).

17. J. P. Winberry, S. Anandakrishnan, D. A. Wiens, R. B. Alley, Nucleation and seismic tremor associated with the glacial earthquakes of Whillans Ice Stream, Antarctica. *Geophys. Res. Lett.* **40**, 312–315 (2013).

18. D. N. Goldberg, C. Schoof, O. V. Sergienko, Stick-slip motion of an Antarctic Ice Stream: The effects of viscoelasticity. *J. Geophys. Res. Earth Surf.* **119**, 1564–1580 (2014).

19. S. Tulaczyk, J. A. Mikucki, M. R. Siegfried, J. C. Priscu, C. G. Barcheck, L. H. Beem, A. Behar, J. Burnett, B. C. Christner, A. T. Fisher, H. A. Fricker, K. D. Mankoff, R. D. Powell, F. Rack, D. Sampson, R. P. Scherer, S. Y. Schwartz, WISSARD at Subglacial Lake Whillans, West Antarctica: Scientific operations and initial observations. *Ann. Glaciol.* **55**, 51–58 (2014).

20. P. J. Bart, S. Tulaczyk, A significant acceleration of ice volume discharge preceded a major retreat of a West Antarctic paleo-ice stream. *Geology* **48**, 313–317 (2020).

21. L. K. Zoet, B. Carpenter, M. Scuderi, R. B. Alley, S. Anandakrishnan, C. Marone, M. Jackson, The effects of entrained debris on the basal sliding stability of a glacier. *J. Geophys. Res. Earth Surf.* **118**, 656–666 (2013).

22. B. P. Lipovsky, C. R. Meyer, L. K. Zoet, C. McCarthy, D. D. Hansen, A. W. Rempel, F. Gimbert, Glacier sliding, seismicity and sediment entrainment. *Ann. Glaciol.* **60**, 182–192 (2019).

23. S. Tulaczyk, B. Kamb, H. F. Engelhardt, Estimates of effective stress beneath a modern West Antarctic ice stream from till preconsolidation and void ratio. *Boreas* **30**, 101–114 (2001).

24. J. Townend, M. D. Zoback, How faulting keeps the crust strong. *Geology* **28**, 399–402 (2000).

25. C. H. Scholz, *The Mechanics of Earthquakes and Faulting* (Cambridge Univ. Press, ed. 3, 2019).

26. A. Dielforder, R. Hetzel, O. Oncken, Megathrust shear force controls mountain height at convergent plate margins. *Nature* **582**, 225–229 (2020).

27. C. G. Barcheck, S. Y. Schwartz, S. Tulaczyk, Icequake streaks linked to potential mega-scale glacial lineations beneath an Antarctic ice stream. *Geology* **48**, 99–102 (2020).

28. L. Freund, *Dynamic Fracture Mechanics* (Cambridge Univ. Press, 1990).

29. S. Ide, G. C. Beroza, D. R. Shelly, T. Uchide, A scaling law for slow earthquakes. *Nature* **447**, 76–79 (2007).

30. Z. Peng, J. Gomberg, An integrated perspective of the continuum between earthquakes and slow-slip phenomena. *Nat. Geosci.* **3**, 599–607 (2010).

31. G. Rogers, H. Dragert, Episodic tremor and slip on the Cascadia subduction zone: The chatter of silent slip. *Science* **300**, 1942–1943 (2003).

32. J. Weertman, Stability of the junction of an ice sheet and an ice shelf. *J. Glaciol.* **13**, 3–11 (1974).

33. C. Ritz, T. L. Edwards, G. Durand, A. J. Payne, V. Peyaud, R. C. A. Hindmarsh, Potential sea-level rise from Antarctic ice-sheet instability constrained by observations. *Nature* **528**, 115–118 (2015).

34. B. R. Parizek, K. Christianson, S. Anandakrishnan, R. B. Alley, R. T. Walker, R. A. Edwards, D. S. Wolfe, G. T. Bertini, S. K. Rinehart, R. A. Bindschadler, S. M. J. Nowicki, Dynamic (in)stability of Thwaites Glacier, West Antarctica. *J. Geophys. Res. Earth Surf.* **118**, 638–655 (2013).

35. T. A. Herring, R. W. King, M. A. Floyd, S. C. Mcclusky, GAMIT Reference Manual: GPS Analysis at MIT, Release 10.6, 16 July 2015 (2015).

Citation: G. Barcheck, E. E. Brodsky, P. M. Fulton, M. A. King, M. R. Siegfried, S. Tulaczyk, Migratory earthquake precursors are dominant on an ice stream fault. *Sci. Adv.* **7**, eabd0105 (2021).